

Plasma Sci. Technol. 20 (2018) 065503 (11pp) https://doi.org/10.1088/2058-6272/aaaa18

Study of plasma-based stable and ultra-wideband electromagnetic wave absorption for stealth application

Xuyang CHEN (陈旭阳)[1], Fangfang SHEN (沈方芳)[1], Yanming LIU (刘彦明)[1], Wei AI (艾炜)[2] and Xiaoping LI (李小平)[1]

[1] School of Aerospace Science and Technology, Xidian University, Xi'an 710071, People's Republic of China
[2] Science and Technology on Space Physics Laboratory, China Academy of Launch Vehicle Technology, Beijing 100076, People's Republic of China

E-mail: xychen@mail.xidian.edu.cn

Received 10 November 2017, revised 19 January 2018
Accepted for publication 22 January 2018
Published 30 April 2018

Abstract

A plasma-based stable, ultra-wideband electromagnetic (EM) wave absorber structure is studied in this paper for stealth applications. The stability is maintained by a multi-layer structure with several plasma layers and dielectric layers distributed alternately. The plasma in each plasma layer is designed to be uniform, whereas it has a discrete nonuniform distribution from the overall view of the structure. The nonuniform distribution of the plasma is the key to obtaining ultra-wideband wave absorption. A discrete Epstein distribution model is put forward to constrain the nonuniform electron density of the plasma layers, by which the wave absorption range is extended to the ultra-wideband. Then, the scattering matrix method (SMM) is employed to analyze the electromagnetic reflection and absorption of the absorber structure. In the simulation, the validation of the proposed structure and model in ultra-wideband EM wave absorption is first illustrated by comparing the nonuniform plasma model with the uniform case. Then, the influence of various parameters on the EM wave reflection of the plasma are simulated and analyzed in detail, verifying the EM wave absorption performance of the absorber. The proposed structure and model are expected to be superior in some realistic applications, such as supersonic aircraft.

Keywords: plasma stealth, ultra wideband, Epstein profile, scattering matrix method (SMM), electromagnetic (EM) wave absorption, stable wave absorption

(Some figures may appear in colour only in the online journal)

1. Introduction

Plasma stealth, as an emerging and attractive technology, has been advancing for decades [1–6]. Using plasma to conceal aircraft, ships, etc, has two advantages compared to traditional stealth techniques: (1) it avoids the loss of aerodynamic shape in the design of the stealth or low-observability vehicle; (2) the plasma can be designed to possess high electromagnetic (EM) wave absorbing power and a wide absorbing frequency band. To date, the studies of plasma on stealth can mainly be classified in two categories: the study of plasma antenna [7–12] and the study of plasma as an EM wave absorber [3, 4, 13–23]. For the former, plasma antennas are attractive because they can be switched on when required to transmit or receive EM waves, and can also be switched off to become a dielectric that is transparent to them. For the latter, the plasma is utilized as a new (and possibly excellent) stealth material instead of traditional stealth materials. In this paper, we focus our study on the latter.

Vidmar [3] analyzed the plasma generated by an ionization source in helium or air at atmospheric pressure, and ascertained that it could be used to absorb EM waves over a

wide band frequency. To be an efficient EM wave absorber, he found that the plasma should have a high electron density near the plasma source and diminish in density with the distance from it. The Epstein profile [3, 24] is utilized by Vidmar to describe the above electron density distribution of plasma. Based on the work of Vidmar [3], Chaudhury and Chaturvedi [13, 14] developed a 3D blob model for the electron density distribution of a 3D plasma generated from the point of a slab. In their model, they combined the Epstein profile in the z-direction (perpendicular to the slab) and the Gaussian distribution in the xy-plane (the plane of the slab). Then, they used the finite-difference time-domain (FDTD) to compute the reduction of the radar cross section (RCS) of the generated plasma blobs, optimizing the parameters for better wave absorption analysis.

Besides the aforementioned Epstein profile and Gaussian distribution, some other plasma distributions have also been studied, including the linear distribution [15], parabolic distribution [15] and sine profile [16]. In addition, some researchers constructed several plasma structures and then studied their EM wave absorption properties. He *et al* [17] studied a semi-ellipsoidal-shaped plasma structure with exponential plasma distributions. Zhang *et al* [18] constructed a model based on capacitively coupled plasma and then studied the relationship between the transmission attenuation and discharge parameters. The above works [3, 13–18] are outstanding and very useful for EM wave absorption or plasma stealth applications. However, they put a lot of emphasis on the interactions between the EM wave and plasma, but ignore the consideration of plasma stability. In detail, the electron distribution of the plasma in the aforementioned works can maintain a stable or quasi-stable state only when static or at low speeds (such as on ships or low-speed aircraft). But for high-speed cases (such as supersonic aircraft, rockets, etc), the plasma distribution appears unstable, and is easily destroyed by the air flow. Even if a dielectric shield can be utilized to protect the plasma, the distribution can also be destroyed by the shield and the maneuvering action of the vehicle.

There are some stable plasma absorption designs [19–21]. Yuan [19] studied a composite material containing uniform plasma and radar-absorbing material for stealth design. Bai [20] analyzed the reflection of obliquely incident waves on the composite material. Xu [21] studied an evaluation scheme of plasma stealth effectiveness for a closed plasma structure. The materials mentioned in the work are sealed by a lossless transparent material on the outer surface and by a perfect electric conductor (PEC) on the floor surface. Thus, it is stable and can be used for supersonic vehicle stealth. However, in their design, the plasma is uniform, corresponding to a fixed and narrower (compared to the nonuniform case [3, 13–18]) absorbing band for EM waves, which shows its limitations in realistic applications.

In this paper, we designed a stable plasma-based ultra-wideband EM wave absorber for stealth applications. To maintain the stability of the plasma distribution, the absorber is designed to contain several plasma layers and dielectric layers which are distributed alternately. In each layer, the plasma is designed to be uniform, but from an overall perspective it is nonuniform. Nonuniform plasma is the key to obtaining ultra-wideband wave absorption. We proposed a discrete Epstein distribution model to constrain the nonuniform electron density distribution of the plasma layers, by which the wave absorption range is extended to the ultra-wideband. The scattering matrix method (SMM) [25, 26] is utilized to analyze the EM reflection and the absorption property of the absorber structure. In the simulation, the proposed nonuniform plasma model is compared with the uniform case first, in order to show the validation of the proposed structure and model in ultra-wideband EM wave absorption. Then, the influence of various parameters on the EM wave reflection of plasma are simulated and analyzed in detail to illustrate the EM wave absorption performance of the absorber.

The remainder of this paper is organized as follows: section 2 shows the design of the multi-layer nonuniform stable plasma absorber, section 3 gives an analysis of the discrete nonuniform electron density distribution of the plasma, section 4 shows the simulations and the corresponding analysis, section 5 gives the discussions, and finally the conclusions are given in section 6.

2. Multi-layer nonuniform stable plasma structure as EM wave absorber

In this paper, we only consider a square plate absorber structure. However, the method and analysis procedure are also suitable for other shapes such as circular boards, rhombi, etc. In actual applications, absorbers with various shapes can be utilized in combination. Figure 1 shows the square plate absorber designed in this paper as a 2D model (figure 1(a)) and 3D model (figure 1(b)).

As can be seen in figures 1(a) and (b), the designed absorber has a multi-layer structure, including the surface layer l_1, plasma layers l_2, l_4, l_6, ..., lossless dielectrics layers l_3, l_5, l_7, ..., floor layer l_p, and plasma generator boards. The floor layer can be designed to be a PEC, and the surface layer should be designed to be a lossless dielectric (the same as the dielectrics layers) in order to make it transparent to the incident EM wave. The plasma layers and dielectric layers are staggered in arrangement. Each plasma layer has the same thickness d_p, and each dielectric layer has the same thickness d_d.

In each plasma layer, its electron density is uniform, but the different layer has a different electron density, forming a discrete nonuniform electron density distribution from the overall view of the absorber. The dielectric layers mainly act as insulators of the neighboring plasma layers with different electron densities. The plasma generator boards lie on two sides of the absorber, as shown in figure 1(b), and their function is to generate plasma with different electron densities for different plasma layers.

Figure 2 shows the structure of one plasma layer. As can be seen, there are two sets of plasma generator arrays in the plasma generator boards, and they produce plasma in the region of the plasma layer, forming a plasma field. The

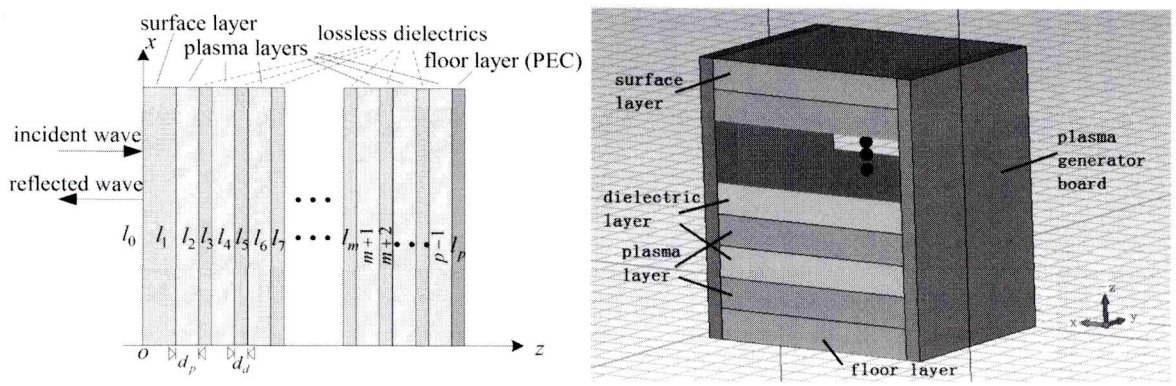

Figure 1. A multi-layer nonuniform stable plasma structure as an EM wave absorber; (a) 2D view in the *xz* plane, (b) 3D view in the *xyz* axes.

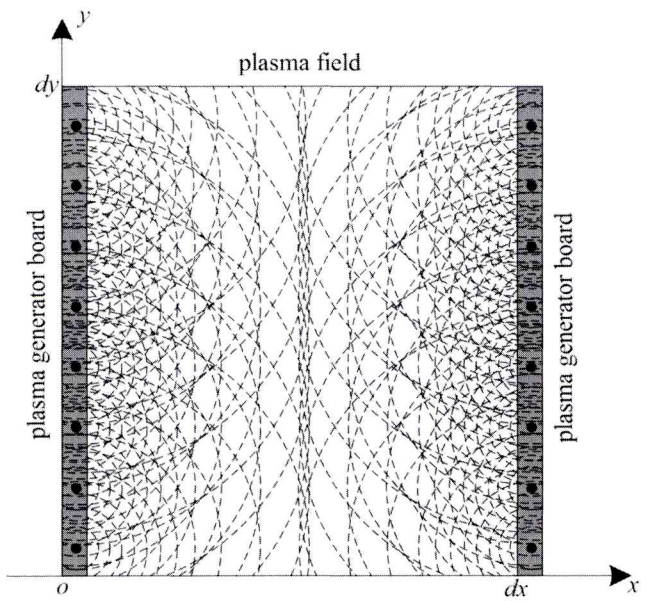

Figure 2. The structure of one plasma layer.

plasma generator can be constructed by an electron-beam source [27, 28]. The spaces between each two neighboring plasma generators in the array are assumed to be much smaller than the location range of the plasma layer, in order that the gradient of the electron density of the plasma along the *y* axis (parallel to the plasma generator array) does not change much.

As for the plasma field in figure 2, it is a scalar field, which describes the superposed distribution of the plasma produced by the plasma generators. The characteristic of the plasma field can mainly be described by the electron density. It is found that each plasma generator in figure 2 produces a set of concentric contour lines (the dashed lines) of electron density. All these concentric contour lines form a superposed electron density distribution. Under the compact arrangement of plasma generators along the direction of the *y* axis, as indicated above, the distribution of the electron density degenerates to a 1D description along the *x* axis, and it is assumed to follow the Epstein profile [3, 13]

$$n_{lm}^{(\mathrm{left})}(x) = \frac{n_{0(lm)}}{1 + \exp(x/L_{lm})}, \quad x \in [0, d_x] \tag{1}$$

where $n_{lm}^{(\mathrm{left})}(x)$ is the electron density distribution of the plasma along the *x* axis in layer l_m generated by the left array in figure 2 (note: supposing l_m is a plasma layer here), d_x is the distance between the two plasma generator arrays, $n_{0(lm)}$ is the electron density basis to be determined and L_{lm} is the distance scale factor to be determined.

Similarly, the electron density distribution $n_{lm}^{(\mathrm{right})}(x)$ of the plasma generated by the right array in figure 2 can be written as

$$n_{lm}^{(\mathrm{right})}(x) = \frac{n_{0(lm)}}{1 + \exp((d_x - x)/L_{lm})}, \quad x \in [0, d_x]. \tag{2}$$

The electron density $n_{lm}^{(\mathrm{all})}(x)$ of the whole plasma field is the superposition of $n_{lm}^{(\mathrm{left})}(x)$ and $n_{lm}^{(\mathrm{right})}(x)$, which can be expressed as follows:

$$n_{lm}^{(\mathrm{all})}(x) = n_{lm}^{(\mathrm{left})}(x) + n_{lm}^{(\mathrm{right})}(x) = \frac{n_{0(lm)}}{1 + \exp(x/L_{lm})} + \frac{n_{0(lm)}}{1 + \exp((d_x - x)/L_{lm})}, x \in [0, d_x]. \tag{3}$$

The electron density in the plasma layer should be of fine uniformity; in other words, the difference between the maximum and the minimum of $n_{lm}^{(\mathrm{all})}(x)$ should be within an acceptable range. By taking the derivative of $n_{lm}^{(\mathrm{all})}(x)$ and setting it to zero, one can obtain the value and position of the minimum of $n_{lm}^{(\mathrm{all})}(x)$, as shown below:

$$n_{lm}^{\mathrm{MIN}} = \frac{2n_{0(lm)}}{1 + \exp\left(\frac{d_x}{2L_{lm}}\right)}, \tag{4a}$$

$$x_{lm}^{\mathrm{MIN}} = \frac{d_x}{2}. \tag{4b}$$

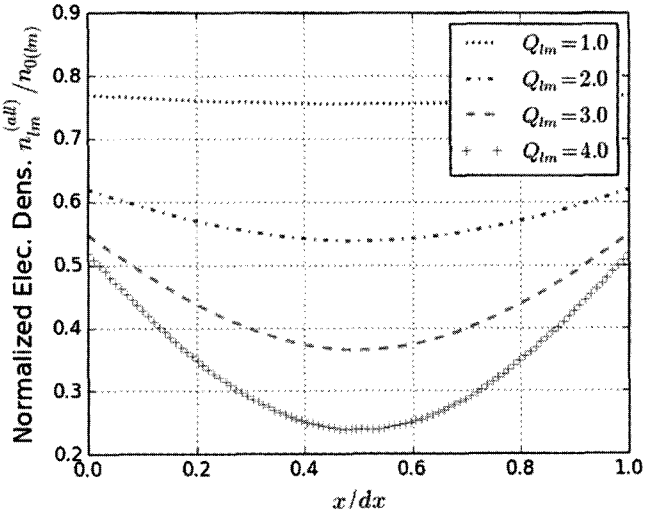

Figure 3. The normalized electron density $n_{lm}^{(\mathrm{all})}(x)/n_{0(lm)}$ versus x/d_x.

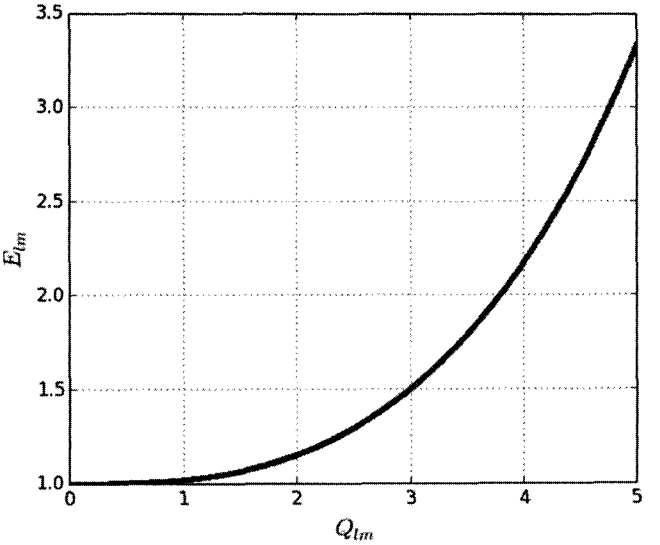

Figure 4. The relation of E_{lm} versus Q_{lm}.

The maximum occurs at the boundary point of the range of x, with its value and positions expressed by

$$n_{lm}^{\mathrm{MAX}} = \frac{n_{0(lm)}\left(\frac{3}{2} + \frac{1}{2}\exp\left(\frac{d_x}{L_{lm}}\right)\right)}{1 + \exp\left(\frac{d_x}{L_{lm}}\right)}, \tag{5a}$$

$$x_{lm}^{\mathrm{MAX}} = 0 \text{ or } d_x. \tag{5b}$$

The ratio of n_{lm}^{MAX} to n_{lm}^{MIN} (denoted by E_{lm}) is used to estimate the uniformity of the plasma, expressed by

$$E_{lm}(Q_{lm}) = \frac{n_{lm}^{\mathrm{MAX}}}{n_{lm}^{\mathrm{MIN}}} = \frac{(\exp(Q_{lm}) + 3)(\exp(Q_{lm}/2) + 1)}{4(\exp(Q_{lm}) + 1)}, \tag{6}$$

where Q_{lm} is defined by

$$Q_{lm} = \frac{d_x}{L_{lm}}. \tag{7}$$

As can be seen in equations (6) and (7), the uniformity of the plasma is only related to Q_{lm}, which is the ratio of the distance between the two plasma generator arrays d_x to the distance scale factor L_{lm}. Figure 3 shows the normalized electron density $n_{lm}^{(\mathrm{all})}(x)/n_{0(lm)}$ versus x/d_x for four different Q_{lm}. Figure 4 shows the numerical relation of E_{lm} versus Q_{lm}.

Clearly, the smaller the Q_{lm}, the flatter the electron density and the better the uniformity of the plasma. If one does not expect the maximum electron density to be twice as big as the minimum electron density—meaning E_{lm} is not larger than two—then Q_{lm} should be designed to be no larger than 3.79, which can be seen in figure 4.

When the size d_x of the absorber is determined, the distance scale factor L_{lm} can then be determined by choosing a smaller E_{lm} and the following equations (6) and (7). The order of the electron density of a plasma layer is controlled by the basis density $n_{0(lm)}$. Once the two terms L_{lm} and $n_{0(lm)}$ are determined, one can obtain the uniform and stable electron density distribution of the plasma layer.

3. Analysis of discrete nonuniform electron density distribution of plasma

In section 2, the multi-layer absorber design is presented, and the parameters for the stable and uniform electron density distribution of the plasma layers are also analyzed. The following work is to determine the discrete electron density distribution of the plasma for the whole absorber.

Since each plasma layer has a uniform plasma electron density distribution, only one symbol can be used to identify the electron density of one plasma layer. Let $\bar{n}_{lm}$ denote the average plasma electron density of layer l_m (here suppose l_m is the plasma layer).

A uniform plasma has a narrower absorbing band for EM waves than nonuniform plasma. This is because a uniform plasma corresponds with a certain plasma frequency ω_{pla}, and only those EM waves with a frequency near ω_{pla} can be absorbed effectively. For those waves with a frequency much higher than ω_{pla}, the plasma acts like a dielectric which is nearly transparent to the waves, whereas for those waves with a much lower frequency than ω_{pla}, the plasma acts like a conductor and thus reflects most of the waves. For the nonuniform plasma case, there is no determined ω_{pla}; instead, there is a broad absorbing frequency region. To obtain an effective ultra-wideband EM wave absorber, the plasma distribution should be designed to be nonuniform as a whole.

The Epstein profile is an effective approximation of the nonuniform plasma distribution and was utilized in section 2. In this section, we develop a discrete form of Epstein profile to construct the discrete plasma distribution of all the plasma layers. The constructed discrete Epstein profile can be expressed as

81

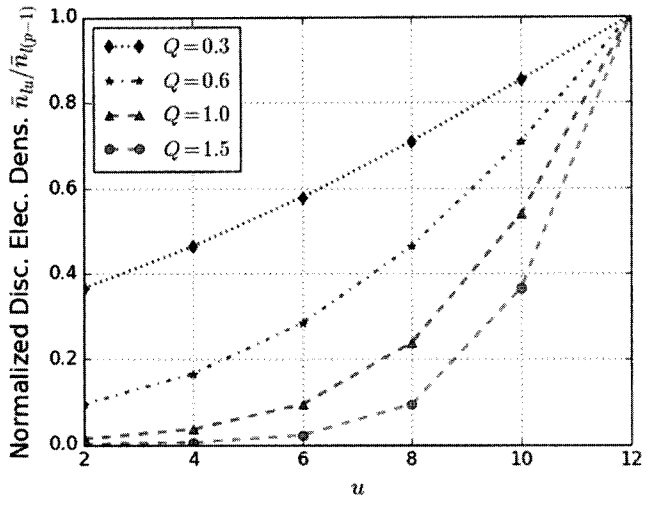

Figure 5. The normalized discrete electron density $\bar{n}_{lu}/\bar{n}_{l(p-1)}$ versus layer index u with $p = 13$.

follows:

$$\bar{n}_{lu} = \frac{2\bar{n}_{l(p-1)}}{1 + \exp\left(\frac{(p-1-u)d_p}{2L}\right)} = \frac{2\bar{n}_{l(p-1)}}{1 + \exp\left(\frac{(p-1-u)Q}{2}\right)},$$
$$u = 2,\ 4,\ 6, ..., p-5,\ p-3,\ p-1 \tag{8}$$

and

$$Q = \frac{d_p}{L} \tag{9}$$

where $\bar{n}_{l(p-1)}$ is the average electron density of plasma layer l_{p-1}, $\bar{n}_{lu}$ is the average electron density of plasma layer l_u, L is the distance scale factor of all the plasma layers (note: it is different from L_{lm} as shown in section 2), and Q is the ratio of d_p to L, which describes the changing rate of the nonuniform plasma. To visually show the discrete electron density distribution, we present an example of the normalized discrete electron density $\bar{n}_{lu}/\bar{n}_{l(p-1)}$ versus the layer index u with $p = 13$ and four selected Q, as plotted in figure 5. It can be seen that a larger Q will result in a sharper discrete electron density distribution.

Once the average electron density $\bar{n}_{l(p-1)}$ and the ratio Q are determined, the whole discrete electron density distribution $\bar{n}_{lu}$ will be decided. To determine $\bar{n}_{l(p-1)}$ and Q requires elaborate parameter design for maximal absorption (or minimal reflection) performance of the EM wave of the absorber. Note that the nonuniform plasma distribution, as shown in equation (8), is expressed in a 1D model. Although the constructed plasma structure in figure 1 is a 3D model, as for the plane EM wave and plane absorber, it can be dimensionally reduced to a 1D model. So the 1D form of equation (8) is reasonable and suitable for describing the plasma distribution of the constructed EM wave absorber. The 1D scattering matrix method (SMM) [25, 26] is an easy and effective way of analyzing the interaction of nonuniform plasma with an EM wave, and it is employed here to analyze the EM properties of the proposed structure.

The SMM divides the nonuniform plasma into several layers, and in any layer the plasma is regarded as uniform. The total reflection and transmission coefficients of the whole nonuniform plasma can be calculated in a cascaded and recursive way on each layer.

The plasma considered in this paper is cold, unmagnetized, nonuniform and collisional, which complies with the constraint of the SMM and thus can be analyzed by it. The structure of figure 1(a) only meets with the stratification structure of SMM and is adopted for SMM analysis.

The propagation coefficient $k^{(m)}$ of layer l_m is expressed as follows:

$$k^{(m)} = \frac{\omega}{c}\sqrt{\varepsilon_r^{(m)}},\ m \in \{0, 1, 2, ..., p\}, \tag{10}$$

where c is the light velocity in a vacuum (m s^{-1}), ω is the frequency of the incident EM wave (rad s^{-1}), and $\varepsilon_r^{(m)}$ is the relative complex dielectric constant of layer l_m.

If l_m is a plasma layer, the parameter $\varepsilon_r^{(m)}$ is co-determined by the plasma frequency $\omega_{pla,m}$ of layer l_m, the collision frequency ν_m of layer l_m, and the incident frequency ω, as expressed below [29]:

$$\varepsilon_r^{(m)} = 1 - \frac{\omega_{pla,m}^2/\omega^2}{1 - j\frac{\nu_m}{\omega}}, \tag{11}$$

where the plasma frequency $\omega_{pla,m}$ can be expressed as follows:

$$\omega_{pla,m} = \sqrt{\frac{\bar{n}_{lm}e^2}{\varepsilon_0 m_e}}, \tag{12}$$

where $\bar{n}_{lm}$ is the average electron density of layer l_m (m^{-3}), e is the electric quantity of an electron (C), m_e is the mass of an electron (kg) and ε_0 is the dielectric constant in a vacuum (F m^{-1}).

If l_m is a dielectric layer, the parameter $\varepsilon_r^{(m)}$ is determined by the material characteristics.

Assume that the polarization direction of the incident wave is $+y$ and its electric field in $z = 0$ is E_0, then one can express the total electric field of the EM wave in an incident region (layer l_0 in figure 1(a)) as follows:

$$E_y^{(0)} = E_0(\exp(-jk_z^{(0)}z) + A\exp(jk_z^{(0)}z)), \tag{13}$$

where A is the total reflection coefficient to be determined.

Note that the time factor $\exp(j\omega t)$ is omitted in equation (13) because it is the same for each term of the equation; it is also omitted by the following relative equations for the same reason.

The total electric field of layer l_m can be expressed by

$$E_y^{(m)} = E_0(B_m\exp[-jk_z^{(m)}z] + C_m\exp(jk_z^{(m)}z)),$$
$$m \in \{1, 2, ..., p\} \tag{14}$$

where B_m and C_m are the transmission coefficient and reflection coefficient of layer l_m, respectively.

The following deductions are the same as those in the SMM procedure, and they are presented in the appendix section. Using the SMM, one can obtain the total reflection coefficient A and the total transmission coefficient D. Because

the floor layer of the plasma structure in figure 1 is a PEC, there is almost no wave to transmit it, so the coefficient D can be ignored here. The energy absorption coefficient P, which describes the energy absorption of the absorber, can then be expressed by

$$P = 1 - |A|^2. \tag{15}$$

After the above deduction, it is necessary to analyze the determination of the average electron density $\bar{n}_{l(p-1)}$ and the ratio Q from a qualitative point of view. To use the EM wave absorber, one should first select a frequency range in which the EM wave can be absorbed by the absorber. For a convenient description, suppose the frequency range is $[f_{\text{low}}, f_{\text{high}}]$ (unit: Hz). The frequency f_{high} corresponds to the plasma frequency $\omega_{\text{pla},p-1}$ of layer l_{p-1}, and then the electron density $\bar{n}_{l(p-1)}$ can be determined by equation (12). For the frequency f_{low}, this corresponds to the plasma frequency $\omega_{\text{pla},2}$ of layer l_2, and the electron density $\bar{n}_{l_2}$ can then be decided by equation (12). For a fixed layer number p and determined parameters $\bar{n}_{l(p-1)}$ and l_2, the ratio Q can be decided by equation (8). For a given plasma layer thickness d_{p}, the distance scale factor L can then be determined. The qualitative analysis above just gives a direction to determine the mentioned parameters, whereas the performance analysis of the absorber and a quantitative analysis should also be taken into consideration in the determination of these parameters. This will need analysis by SMM, and the simulations are shown as follows.

4. Simulations and analysis

In the simulation, we will give the validation of the proposed EM wave absorber structure and the discrete nonuniform electron density distribution model of the plasma. The magnitude of the reflection coefficient of the plasma is utilized to estimate the absorption performance of the absorber. Clearly, the lower the reflection magnitude, the more EM wave energy is absorbed by the plasma. We first give a comparison of the nonuniform model and the uniform model in EM wave absorption in section 4.1, in order to illustrate the validation of the proposed absorber structure and model. Then, we simulate and analyze the influence of various parameters on the absorption performance of the absorber.

The simulation hardware and software settings are shown as follows: CPU: Intel i5 Dual Cores both at 3.3 GHz, memory: 8 GB, OS: Windows 7 (64-bit), and simulation software: Python 2.7.6.

4.1. EM wave absorption—comparison of the nonuniform model with uniform model

In order to illustrate the validation of the proposed discrete nonuniform model, we compared it to the uniform one. To make the comparison fair and believable, the conditions of the two models are set to be the same except for plasma distribution. The structure in figure 1 is selected as the EM wave absorber for both models.

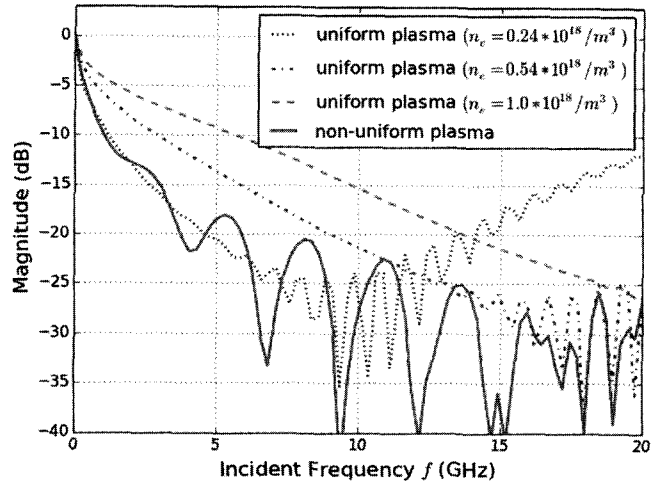

Figure 6. The magnitude of the reflection coefficients of plasma versus the incident frequency f of EM waves for the nonuniform plasma model and three uniform plasma cases.

The parameters of the absorber are set as follows: the thickness of the surface layer is set to be 0.01 m, the thickness of the inner chamber of the absorber structure (from the inner surface of the surface layer to the inner surface of the floor layer) is 0.166 m. The material of the inner dielectric layers (only needed by the nonuniform plasma case) and that of the surface layer are considered to be lossless dielectrics here (corresponding to the relative dielectric constant $\varepsilon_{\text{r}} = 1$). The floor layer is a PEC. As for the size of each plasma layer, it is not involved in the calculation and thus not given here. As for the plasma, the collision frequency ν for all plasma layers is set to be 10 GHz both for the uniform and nonuniform case. The frequency analysis range for the EM wave is set to be 1 MHz–20 GHz in steps of 0.25 GHz.

For the nonuniform plasma model, the thicknesses of the inner layers are set as follows: $d_{\text{p}} = 0.05$ m, $d_{\text{d}} = 0.008$ m, and the layer number parameter $p = 7$ (including three plasma layers and two inner dielectric layers). The above setting guarantees the total thickness of the inner chamber to be $3d_{\text{p}} + 2d_{\text{d}} = 0.166$ m. The ratio Q is set to be 1, and the average electron density of layer l_{p-1} is $\bar{n}_{l(p-1)} = 1.0 \times 10^{18}\,\text{m}^{-3}$. Under the above setting, applying the discrete Epstein distribution, as shown in equation (8), one can obtain three plasma electron densities for the three plasma layers: $\bar{n}_{l_2} = 0.24 \times 10^{18}\,\text{m}^{-3}$, $\bar{n}_{l_4} = 0.54 \times 10^{18}\,\text{m}^{-3}$, and $\bar{n}_{l_6} = 1.0 \times 10^{18}\,\text{m}^{-3}$.

For the uniform plasma model, there is only one uniform plasma layer with $d_{\text{p}} = 0.166$ m, but without an inner dielectric layer ($d_{\text{d}} = 0$ and $p = 3$). For comparison, three plasma electron density cases are tested: $0.24 \times 10^{18}\,\text{m}^{-3}$, $0.54 \times 10^{18}\,\text{m}^{-3}$ and $1.0 \times 10^{18}\,\text{m}^{-3}$, respectively.

The SMM is utilized to simulate the reflection coefficients of the plasma for the nonuniform and uniform model, with the result shown in figure 6. The symbol n_{e} in the legend of the figure denotes the electron density of the plasma. As shown in figure 6, the uniform plasma with $n_{\text{e}} = 0.24 \times 10^{18}\,\text{m}^{-3}$ has a

85

relatively fine reflection attenuation performance (or absorption performance) for a frequency f lower than about 10 GHz, but the reflection becomes enhanced when f is larger than 10 GHz. However, the case with $n_e = 1.0 \times 10^{18}\,\mathrm{m}^{-3}$ has an acceptable reflection attenuation for a frequency f larger than about 14 GHz. The case with $n_e = 0.54 \times 10^{18}\,\mathrm{m}^{-3}$ is a compromise of the other two uniform cases. The result of the nonuniform plasma model, however, has outstanding reflection attenuation in the whole frequency analysis range compared to all three uniform plasma cases.

The reason for the outstanding wave absorption of the nonuniform plasma model can be analyzed as follows. According to the discrete Epstein distribution, as shown in equation (8), the electron density of plasma is highest near the floor layer, and it falls off with the decreasing index number of the plasma layers. In this simulation, the plasma layer l_2 has the lowest electron density $0.24 \times 10^{18}\,\mathrm{m}^{-3}$, and it absorbs the EM waves significantly for f lower than 10 GHz. For those waves with a higher f (larger than 10 GHz here), some of them will also be absorbed, but those that are left will penetrate layer l_2 and get into layer l_4. In layer l_4, the plasma possesses a better absorption performance than l_2 for higher f frequencies, and it absorbs most of the penetrated waves; however, it also misses a very small number of waves with much higher f frequencies. These rare missed waves will penetrate layer l_6, where the absorption power is much higher than layer l_4 for waves with much higher frequencies, and these waves are absorbed significantly.

It should be noticed that the nonuniform design cannot be reversed. If one sets l_2 to possess the highest electron density and sets l_6 to have the lowest, many of the incident waves with lower frequencies will be reflected directly but not penetrate the other inner layers.

The simulation of this section has shown the validation of the proposed nonuniform plasma model in EM wave absorption. In the next sections, we will illustrate the influence of various parameters and find the influence rules.

4.2. Influence of various parameters on EM wave absorption

4.2.1. Influence of Q. The parameter Q denotes the ratio of d_p to L, and it is an important parameter in the proposed nonuniform plasma model. Q reflects the changing rate of the discrete nonuniform plasma. The larger the Q, the larger the change of the electron density of the plasma from layer l_2 to l_{p-1}.

In the simulation of this section, let Q change from 0.1 to 1.5 in steps of 0.075; the electron density of the plasma in layer l_{p-1} is $1.0 \times 10^{18}\,\mathrm{m}^{-3}$. All the other parameters are the same as that in section 4.1. The magnitude of the reflection coefficient of the plasma with changing Q and incident frequency f are simulated, with the result shown in figure 7.

As can be seen from figure 7, with the increase of Q, the left boundary of the attenuation range of the frequency shifts towards the lower frequency, enlarging the whole attenuation range. Due to this property, a 'ridge' is formed, which is shown in the figure. Below the 'ridge', the reflection is large,

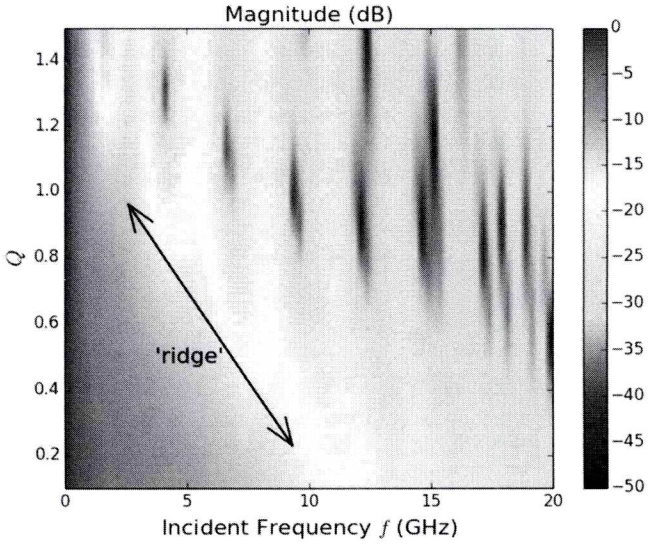

Figure 7. The magnitude of reflection coefficients of plasma versus Q and the incident frequency f.

whereas above the 'ridge', the reflection is attenuated. The 'ridge' characteristic can be explained by the range of electron density of the plasma, which is influenced by Q. As indicated by equation (8), a larger Q results in the extension of the lower boundary of the electron density $\bar{n}_{lu}$ toward lower frequencies, which further leads to a lower plasma frequency $\omega_{\mathrm{pla},m}$ in equation (12) and causes the extension of the absorbing boundary to lower frequencies. However, a larger Q will not influence the upper boundary of the electron density, which is only determined by the quantity $\bar{n}_{l(p-1)}$, as shown in equation (8). Thus, a 'ridge' is formed toward the lower frequencies with the increase of Q, as illustrated in figure 7. In realistic applications, when the absorption range of the EM wave in the frequency is determined, one can select a suitable Q to fit the range.

4.2.2. Influence of d_p/d_d. The value d_p/d_d is the ratio of plasma layer thickness to dielectric layer thickness, and its influence on the reflection coefficients can provide help to determine the optimal d_p and d_d. Let d_p/d_d vary from 0.1 to 10 in steps of 0.1 and let the inner thickness of the chamber be 0.166 m. The other parameters are the same as those in section 4.1 except for the values d_p and d_d, which are both determined by the ratio d_p/d_d and the fixed inner chamber thickness. The simulation result is shown in figure 8.

From figure 8, one can see that the magnitude of reflection coefficients is large for all ranges of f when d_p/d_d is at a significantly low value, but it will decline rapidly when d_p/d_d increases. The threshold value of d_p/d_d can be seen in figure 8, and is about 1.7 here (for the frequency range 1 MHz–20 GHz). When the ratio d_p/d_d increases over the threshold, the reflection magnitude will almost keep a stable distribution for the whole range of f, with the attenuation region unaltered. According to further tests, this threshold is very robust, and nearly remains unchanged with variation of

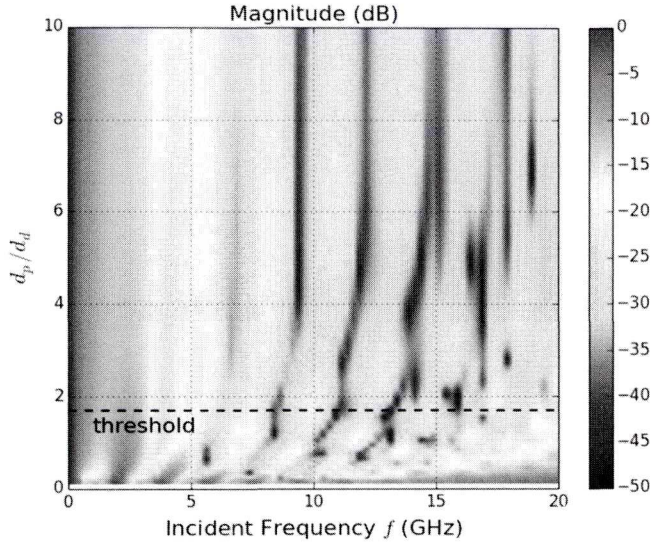

Figure 8. The magnitude of the reflection coefficients of the plasma versus d_p/d_d and the incident frequency f.

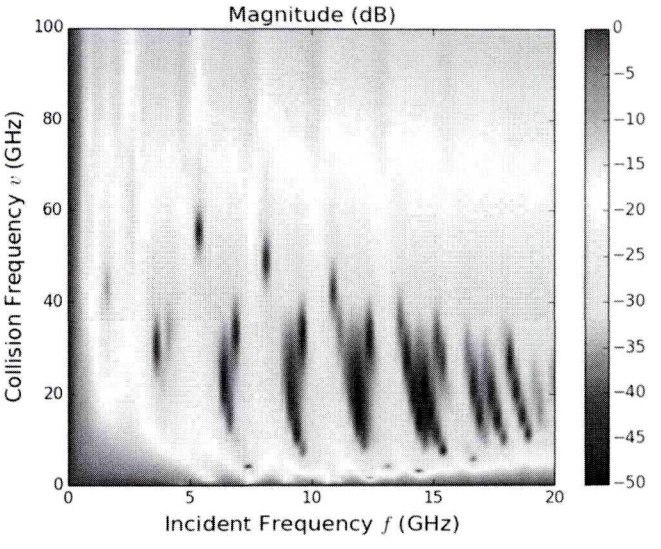

Figure 9. The magnitude of the reflection coefficients of plasma versus the collision frequency v and incident frequency f.

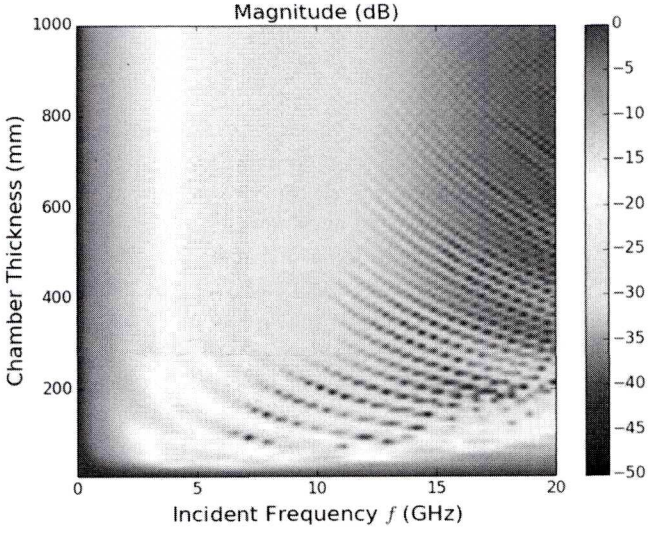

Figure 10. The magnitude of the reflection coefficients of plasma versus chamber thickness and incident frequency f.

the other parameters. It also reflects the robust distribution of the reflection coefficients versus d_p/d_d.

The changing rule of reflection magnitude along with d_p/d_d shown in figure 8 is not difficult to understand. The fixed chamber thickness in this section limits the maximal plasma thickness. At the beginning of the increase of d_p/d_d, the increased plasma thickness absorbs more EM waves, leading to a rapid reduction of the reflection magnitude. However, as d_p/d_d continues to increase, the thickness of the plasma increases slowly due to the fixed chamber thickness, resulting in a slow change of reflection magnitude. In realistic applications, under a selected frequency analysis range, one can find out the changing threshold of the reflection magnitude as mentioned above, based on which the two values d_p and d_d in the region d_p/d_d over the threshold can then be determined.

4.2.3. Influence of collision frequency ν and chamber thickness. The collision frequency v of the plasma and the inner chamber thickness can both influence the whole absorption property of the plasma, whereas they behave differently for the absorption of plasma. For the collision frequency v, let it change from 0.1 GHz to 100 GHz in steps of 0.1 GHz, with the other parameters the same as that in section 4.1. For the chamber thickness, let it vary from 0.01 m to 1 m in steps of 0.01 m, with a d_p/d_d ratio of 6.25 (the same as that in section 4.1), and the other parameters the same as those in section 4.1. Figures 9 and 10 show the influence of the collision frequency v and chamber thickness on the magnitude of reflection coefficients, respectively.

As can be seen in figure 9, the changing of the collision frequency can be separated by two segments. For the first one, with the increase of collision frequency v from 0.1 GHz to about 40 GHz, the reflection magnitude decreases on the whole. For the second segment, however, when v continues to increase from 40 GHz to 100 GHz, the whole reflection magnitude is enhanced. The increase of the collision frequency means that the collisions of ions and electrons occur more frequently, increasing the energy absorption of EM waves and thus reducing wave reflection. However, when the collision frequency increases to a significantly high state (such as over 40 GHz here), the extremely frequent collisions of particles will prevent a part of the waves from penetrating the plasma, leading to enhanced reflection.

As a comparison, figure 10 shows the influence of chamber thickness on the reflection coefficients. It is clear that the influence of chamber thickness is simple. Along with the increase of the chamber thickness, the reflection of the absorber decreases gradually. It should be noted that the decrease rate is higher at first (corresponding to the thinner thickness of the chamber), whereas it becomes lower for a thicker thickness. In actual applications, one should select a suitable chamber

81

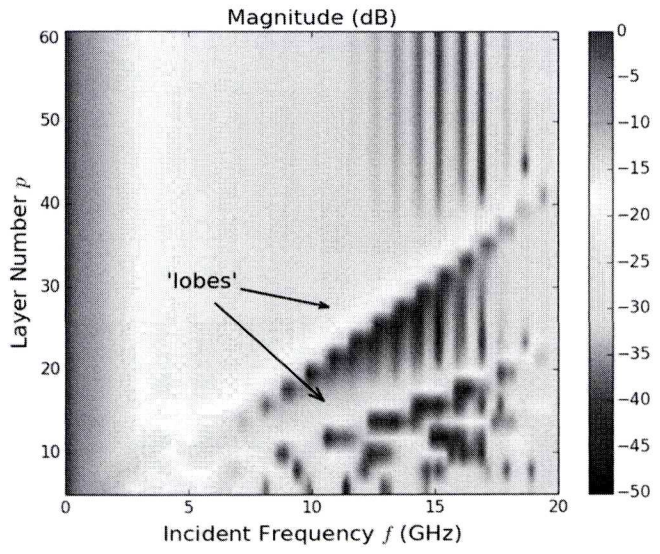

Figure 11. The magnitude of the plasma reflection coefficients versus the layer number p and incident frequency f.

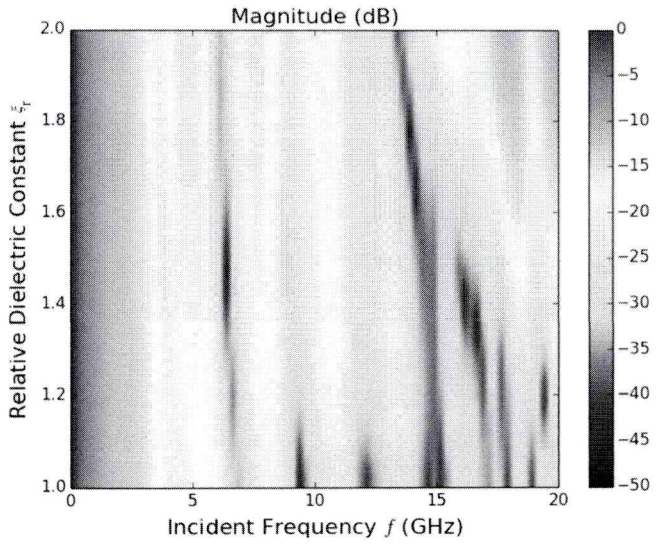

Figure 12. Magnitude of the reflection coefficients of plasma versus the relative dielectric constant ε_r and incident frequency f.

thickness considering a trade-off of absorption performance and physical size.

4.2.4. Influence of the layer number p. The influence of the layer number p on the absorption performance should also be considered. The chamber thickness is set to be 0.166 m and the ratio $d_p/d_d = 6.25$. To avoid the influence of a different range of electron density for a different p, a new parameter $Q_{new} = 4Q/(p-3)$ is used to replace Q in the calculation of $\bar{n}_{lu}$ of equation (8) here, by which the range from $\bar{n}_{l_2}$ to $\bar{n}_{l_{p-1}}$ is the same for each p. Then, let p vary from 5 to 61 in steps of 2 (note: p should be odd). The unmentioned parameters are set the same as those in section 4.1. The simulation result is shown in figure 11.

As can be seen in figure 11, the parameter p mainly affects the positions of the lobes in the frequency axis. With the increase of p, the lobes shift to a higher frequency gradually. The shifting of the lobes is mainly due to the changing state of the phase superposition of the EM waves caused by the variation of the layer number p. Except for the lobes, the influence of p on the total reflection magnitude is small. Usually, p should not be designed to be too large for the simplicity of the structure.

4.2.5. Influence of relative dielectric constant ε_r. In this section, the influence of the relative dielectric constant ε_r of the inner dielectric layers on the reflection magnitude is studied. Let ε_r change from 1.0 to 2.0 in steps of 0.05, where the other parameters are the same as those in section 4.1. Figure 12 shows the simulation result. Clearly, the reflection magnitude is enhanced gradually with an increasing ε_r. According to our analysis, the enhanced reflection magnitude mainly comes from those waves with frequencies higher than the plasma frequencies $\omega_{pla,m}$, which are more easily reflected at the inner interfaces of the plasma structure due to the mismatch caused by the larger ε_r. To minimize the reflection magnitude and further enhance the EM wave absorption, the relative dielectric constant ε_r should be set as small as possible in realistic applications.

5. Discussions

This paper presents a plasma-based EM wave absorber structure and a discrete nonuniform electron distribution model of plasma. Following the design procedure and model of this paper, associated with the proper parameter setting and material selection, one can probably design a wave absorber with acceptable performance. From the above simulations, the reflection attenuation of the EM waves can reach a level of about 20 dB. It would be possible to improve this value with elaborate parameter settings. In addition, in the simulations, the incident frequency range from 1 MHz–20 GHz is considered, which covers most radar applications. Furthermore, the simulation procedure is suitable for any incident frequency range, and one can make new simulations again using the above procedure according to the required frequency range in practical applications.

Besides these situations, a condition should also be indicated. This paper focuses a lot on theoretical analysis, whereas when the structure and model are utilized in applications, realistic engineering problems should also be taken into consideration for the structure design.

One realistic aspect that needs attention is the balance between EM wave absorption performance and power supply. As shown in section 4, the thicker the absorber, the more EM waves it absorbs. To obtain excellent EM wave absorbing performance, the average electron density of the plasma should be set as large as possible. However, the larger volume and higher electron density of the plasma imply larger amounts of desired power, which increases the burden of the carrier (vehicle, shuttle, etc). There are some feasible ways in which realistic applications can decrease the power supply

without loss of EM wave absorbing performance. Noble gases (such as helium) can be used as the host gas for plasma generation as an alternative to air. This gas has a significantly longer lifetime [3] than air and thus decreases the power supply to a great extent. Apart from this, one should consider shielding only the key portions of the object with the plasma structure instead of the whole shell of the object, thus also reducing the power supply.

Another realistic aspect is the choice of materials from which to construct the absorber. The involved portions contain dielectric layers and plasma generation boards. For the dielectric layers, their relative dielectric constants should be as small as possible. Suitable materials can be found among plastic compounds and cokes. To some extent, the plasma generation boards should have anti-compression properties to resist the atmosphere, and they should also have some EM wave absorbing ability. One could consider polymeric matrices or artificial dielectrics [30] to construct the boards.

The plasma-based EM wave absorber is a new and emerging technology, and it will face many challenges in realistic applications; even so, its application prospects and values are attractive.

6. Conclusions

In this paper, we studied a plasma-based stable, ultra-wideband EM wave absorber structure and then proposed a discrete nonuniform electron density distribution model using an Epstein profile for ultra-wideband wave absorption. The SMM is employed to analyze the reflection and absorption property of the plasma-based structure. In the theoretical deductions, two key parameters, Q_{lm} and Q, are derived, which determine the uniformity of each plasma layer and the absorbing band of the EM wave, respectively. In the simulation, by comparing the nonuniform model with the uniform one, the validation of the proposed nonuniform model for ultra-wideband wave absorption is illustrated. Then, elaborate simulations and analyses of the influences of various parameters on the EM wave reflection of plasma are executed. The simulation results will be helpful in guiding the realistic applications of the plasma absorber. In our further work, the obliquely incident case will be considered, and realistic engineering problems in applying the absorber will also be taken into account systematically.

Acknowledgments

This work was supported in part by the National Basic Research Program of China (grant no. 2014CB340205), in part by the Science and Technology on Space Physics Laboratory Funds, and in part by the Fundamental Research Funds for the Central Universities (20101156180).

Appendix. Scattering matrix method (SMM)

SMM [25] is a method used for analyzing the interaction of EM waves with nonuniform plasma in a stratification plasma structure, as shown in figure 1(a). The relative parameters include the plasma frequency $\omega_{p,m}$, the propagation coefficient $k_z^{(m)}$, the electric field $E_y^{(0)}(z)$, the transmission coefficients B_m and the reflection coefficients C_m. All these parameters have been defined in section 3.

The coefficients B_m and C_m satisfy a boundary condition [25, 31] as shown below,

$$\begin{cases} B_m \exp(-\mathrm{j}k_z^{(m)} z_m) + C_m \exp(\mathrm{j}k_z^{(m)} z_m) = B_{m-1} \exp(-\mathrm{j}k_z^{(m-1)} z_m) + C_{m-1} \exp(\mathrm{j}k_z^{(m-1)} z_m) \\ k_z^{(m)} B_m \exp(-\mathrm{j}k_z^{(m)} z_m) - k_z^{(m)} C_m \exp(\mathrm{j}k_z^{(m)} z_m) = k_z^{(m-1)} B_{m-1} \exp(-\mathrm{j}k_z^{(m-1)} z_m) - k_z^{(m-1)} C_{m-1} \exp(\mathrm{j}k_z^{(m-1)} z_m) \\ m \in \{1, 2, ..., p\} \end{cases} \tag{A1}$$

where z_m is the coordinate on the z-axis of the outer surface of layer l_m. Note: $z_1 = 0$.

Equation (A1) can be represented by a matrix form as follows:

$$\begin{pmatrix} B_m \\ C_m \end{pmatrix} = \boldsymbol{S_m} \begin{pmatrix} B_{m-1} \\ C_{m-1} \end{pmatrix}, \ m \in \{1, 2, \ldots, p\}. \tag{A2}$$

The matrix $\boldsymbol{S_m}$ of layer l_m is expressed by

$$\boldsymbol{S_m} = \begin{pmatrix} \exp(-\mathrm{j}k_z^{(m)} z_m) & \exp(\mathrm{j}k_z^{(m)} z_m) \\ k_z^{(m)} \exp(-\mathrm{j}k_z^{(m)} z_m) & -k_z^{(m)} \exp(\mathrm{j}k_z^{(m)} z_m) \end{pmatrix}^{-1} \times \begin{pmatrix} \exp(-\mathrm{j}k_z^{(m-1)} z_m) & \exp(\mathrm{j}k_z^{(m-1)} z_m) \\ k_z^{(m-1)} \exp(-\mathrm{j}k_z^{(m-1)} z_m) & -k_z^{(m-1)} \exp(\mathrm{j}k_z^{(m-1)} z_m) \end{pmatrix}. \tag{A3}$$

The assumption for the boundary layers in equation (A2) is shown below

$$\begin{cases} d_0 = 0, B_0 = 1, C_0 = A & \text{for layer } l_0 \\ B_p = D, C_p = 0 & \text{for layer } l_p \end{cases} \tag{A4}$$

where D is the total transmission coefficient.

Equation (A2) can be expanded as a cascade expression as follows

$$\begin{pmatrix} 1 \\ 0 \end{pmatrix} D = \boldsymbol{S_p S_{p-1} S_{p-2} \ldots S_2 S_1} \begin{pmatrix} 1 \\ A \end{pmatrix}. \tag{A5}$$

By converting equation (A5), one can obtain

$$\boldsymbol{V}_p D = \boldsymbol{S}_g \begin{pmatrix} 1 \\ A \end{pmatrix} \tag{A6}$$

where

$$\boldsymbol{V}_p = \boldsymbol{S}_p^{-1} \begin{pmatrix} 1 \\ 0 \end{pmatrix} = \frac{1}{2k_z^{(p-1)}} \times \begin{pmatrix} (k_z^{p-1} + k_z^p)\exp(\mathrm{j}(k_z^{p-1} - k_z^p)z_p) \\ (k_z^{p-1} - k_z^p)\exp(-\mathrm{j}(k_z^{p-1} + k_z^p)z_p) \end{pmatrix} \tag{A7}$$

and

$$\boldsymbol{S}_g = \prod_{m=p-1}^{1} \boldsymbol{S}_m. \tag{A8}$$

Rewriting matrix $\boldsymbol{S}_g$ as $\boldsymbol{S}_g = \begin{bmatrix} \boldsymbol{S}_{g1} & \boldsymbol{S}_{g2} \end{bmatrix}$ and deforming equation (A6), one can solve the total reflection coefficient A and the total transmission coefficient D by

$$\begin{pmatrix} A \\ D \end{pmatrix} = -\begin{pmatrix} \boldsymbol{S}_{g2} & -\boldsymbol{V}_p \end{pmatrix}^{-1} \boldsymbol{S}_{g1}. \tag{A9}$$

ORCID iDs

Xuyang CHEN (陈旭阳) https://orcid.org/0000-0003-3142-5338

References

[1] Singh H, Antony S and Jha R M 2016 *Plasma-Based Radar Cross Section Reduction* (Singapore: Springer) (https://doi.org/10.1007/978-981-287-760-4)

[2] Vidmar R J 1990 Plasma cloaking: air chemistry, broadband absorption and plasma generation *Report* F49620-85-K-0013 AFOSR (Air Force Office of Scientific Research, USAF)

[3] Vidmar R J 1990 *IEEE Trans. Plasma Sci.* **18** 733

[4] Stalder K R, Vidmar R J and Eckstrom D J 1993 *J. Appl. Phys.* **72** 5089

[5] Yang H W and Liu Y 2010 *J. Infrared Millim. Terahertz Waves* **31** 1075

[6] Ma L X, Zhang H and Zhang C X 2008 *J. Electromagnet. Waves Appl.* **22** 2285

[7] Chung M *et al* 2008 Capacitive coupling return loss of a new pre-ionized monopole plasma antenna *Proceedings of 2007 IEEE Region 10 Conference* (Taipei, Taiwan: IEEE) p 1

[8] Alexeff I *et al* 2008 *Phys. Plasmas* **15** 057104

[9] Kumar R and Bora D 2011 *J. Appl. Phys.* **109** 063303

[10] Barro O A, Himdi M and Lafond O 2016 *IEEE Antennas Wirel. Propag. Lett.* **15** 726

[11] Ramli N F, Dagang A N and Ali M T 2015 Analysis of reconfigurable line pattern of capillary plasma antenna array *AIP Conf. Proc.* **1657** 150005

[12] Théberge F *et al* 2017 *Appl. Phys. Lett.* **111** 073501

[13] Chaudhury B and Chaturvedi S 2005 *IEEE Trans. Plasma Sci.* **33** 2027

[14] Chaudhury B and Chaturvedi S 2009 *IEEE Trans. Plasma Sci.* **37** 2116

[15] Cheng D and Zheng H X 2015 Study on electromagnetic scattering of perfectly conducting cylinder coated with nonuniform isotropic plasma *Proc. of the 8th Int. Conf. on Intelligent Networks and Intelligent Systems* (Tianjin, China: IEEE) p 161

[16] Liu S H and Guo L X 2016 *IEEE Trans. Plasma Sci.* **44** 2838

[17] He X *et al* 2015 *Plasma Sci. Technol.* **17** 869

[18] Zhang Y C *et al* 2017 *Phys. Plasmas* **24** 083511

[19] Yuan C X *et al* 2011 *IEEE Trans. Plasma Sci.* **39** 1768

[20] Bai B W *et al* 2015 *IEEE Trans. Plasma Sci.* **43** 2558

[21] Xu J *et al* 2017 *IEEE Trans. Plasma Sci.* **45** 938

[22] Ma L X *et al* 2010 Analysis on the refraction stealth characteristic of cylinder plasma envelopes *Proc. of 2010 Int. Conf. on Microwave and Millimeter Wave Technology* (Chengdu, China: IEEE) p 1695

[23] Wang G *et al* 2009 RCS calculation of complex targets shielded with plasma based on visual GRECO method *Proceedings of the 3rd IEEE International Microwave, Antenna, Propagation and EMC Technologies for Wireless Communications* (Beijing, China: IEEE) p 950

[24] Budden K G 1985 *The Propagation of Radio Waves: The Theory of Radio Waves of Low Power in the Ionosphere and Magnetosphere* (Cambridge, UK: Cambridge University Press)

[25] Hu B J, Wei G and Lai S L 1999 *IEEE Trans. Plasma Sci.* **27** 1131

[26] Soliman E A, Helaly A and Megahed A A 2007 *Prog. Electromagn. Res.* **67** 25

[27] Fernsler R F *et al* 1998 *Phys. Plasmas* **5** 2137

[28] Macheret S O, Shneider M N and Miles R B 2001 *Phys. Plasmas* **8** 1518

[29] Heald M A and Wharton C B 1965 *Plasma Diagnostics with Microwaves* (New York: Wiley)

[30] Kumar N E and Vadera S R 2017 Stealth materials and technology for airborne systems ed N Prasad and R Wanhill *Aerospace Materials and Material Technologies* (Singapore: Springer)

[31] Chew W C 1995 *Waves and Fields in Inhomogeneous Media* (New York: IEEE Press)